Polymer Testing 69 (2018) 26–31

Contents lists available at ScienceDirect

Polymer Testing

journal homepage: www.elsevier.com/locate/polytest

Material Performance

Water based scintillator ink for printed X-ray radiation detectors

J. Oliveira[a,b,*], P.M. Martins[a,c], V. Correia[a,b], L. Hilliou[d], D. Petrovykh[e], S. Lanceros-Mendez[f,g,**]

[a] Centre/Departament of Physics, University of Minho, Campus de Gualtar, 4710-057 Braga, Portugal
[b] Algoritmi Research Center, Universidade do Minho, Campus de Azurém, 4800-058 Guimarães, Portugal
[c] CEB - Centre of Biological Engineering, University of Minho, 4710-057 Braga, Portugal
[d] Institute for Polymers and Composites/i3N, Universidade do Minho, 4800-058 Guimarães, Portugal
[e] International Iberian Nanotechnology Laboratory INL, Av. Mestre Jose Veiga, 4710-057 Braga, Portugal
[f] BCMaterials, Basque Center for Materials, Applications and Nanostructures, UPV/EHU Science Park, 48940 Leioa, Spain
[g] IKERBASQUE, Basque Foundation for Science, 48013 Bilbao, Spain

ARTICLE INFO

Keywords:
Printed technologies
Polymer nanocomposites
Photodetector
Scintillator nanocomposites
Water soluble polymers
X-ray detectors

ABSTRACT

Environmentally-friendly materials are being pursued world-wide for applications across a wide range of technologies. For application in spray-printed radiation detectors, water-based scintillator inks have been produced by combining a thermoplastic elastomer poly (vinyl) alcohol (PVA) and $Gd_2O_3:Eu^{3+}$ scintillator nanoparticles. Formulations of these green inks with different concentrations of scintillator nanoparticles have been assessed in terms of their rheological properties: the optimal concentration of scintillator nanoparticles in the water-based ink for spray-printing was 0.75 wt%. This optimized ink formulation exhibits Newtonian behavior with a viscosity around 100 cps and performance characteristics suitable for spray-printing scintillators for indirect X-ray detectors.

1. Introduction

Printing and other additive manufacturing processes are increasingly being used in technological applications [1]. The success of these processes is dependent on providing an environmentally-friendly, low-cost and practical method for the fabrication of tailored flexible and disposable structures and devices, including electronic and biomedical devices [2–4].

X-ray detectors are among the biomedical sensors that can benefit from recent developments in materials and fabrication techniques. Applications of traditional X-ray detectors in medical imaging are limited by the low mechanical flexibility and high cost of bulk scintillators [5,6]. In contrast, polymer-based scintillator composites [7] now offer such beneficial properties as short scintillation decay time, extended thermal stability, mechanical and chemical stability [6,8], low cost and simple fabrication into large areas or complex (compliant) shapes [9].

High efficiency and fast time response have been demonstrated for advanced polymer-based X-ray detectors [10]. Polymer composites with scintillator particles provide additional benefits for radiation detection in many applications [11–14], due to the combination of the low cost of the polymer matrix and the contribution of the particles to the increase of composite density and atomic number [15].

These types of functional composite materials can be implemented using printing technologies with inks appropriately designed [16] to take advantage of the wide range of physicochemical properties and extensive possibilities for tailoring functional properties of the polymer component of the ink [17,18]. Radiation detectors can be printed using techniques such as spray- or screen-printing to produce low-cost flexible sensors and devices [19,20]. Spray-printing in particular is a low-cost process for producing polymer coatings [21] with a distribution of ink sufficiently uniform to be compatible with large-area printed electronics [22]. Most of the polymers used for printing technologies are, however, processed from solutions in toxic solvents, creating environmental hazards and critical problems for biomedical applications [23]. Water-based polymer inks would, therefore, be desirable for printed-sensor applications of polymer-matrix composites.

Poly (vinyl alcohol) (PVA) is a suitable polymer in this context, being water-soluble, biocompatible, biodegradable, and thus commonly used in biomedical devices, drug delivery and food packaging industries [24,25]. The use of PVA in sensor applications also takes advantage of its chemical resistance [24] and mechanical properties [26,27].

The beneficial properties of PVA as a polymer matrix can be complemented in a composite material by scintillator nanoparticles of europium-doped (3 wt%) gadolinium oxide, $Gd_2O_3:Eu^{3+}$ (hereafter GDO), with a particle size of around 30 nm, which exhibits a wide band

* Corresponding author. Centre/Departament of Physics, University of Minho, Campus de Gualtar, 4710-057 Braga, Portugal.
** Corresponding author. BCMaterials, Basque Center for Materials, Applications and Nanostructures, UPV/EHU Science Park, 48940 Leioa, Spain.
E-mail addresses: joliveira@fisica.uminho.pt (J. Oliveira), senentxu.lanceros@bcmaterials.net (S. Lanceros-Mendez).

https://doi.org/10.1016/j.polymertesting.2018.04.042
Received 9 March 2018; Accepted 28 April 2018
Available online 05 May 2018
0142-9418/

gap (≈5.2 eV), high atomic number, high density (≈7.4 g cm^{-3}), suitable light yield (~2 × 10^4 photons·MeV^{-1}) and radioluminescence [28]. Furthermore, fluorescence molecules 2,5 diphenyloxazol (PPO) and (1,4-bis (2-(5-phenioxazolil))-benzol (POPOP) can be used to increase the visible light yield efficiency [29,30], particularly in combination with GDO dispersed in a polymer matrix [31,32].

Accordingly, a new scintillator ink based on PVA together with scintillator GDO nanoparticles and PPO and POPOP fluorescence molecules is reported here as a critical enabling step for spray-printing X-ray detectors constructed from water-based polymer composite materials able to convert X-ray radiation into visible light.

2. Experimental

2.1. Materials

Poly (vinyl alcohol), PVA, 98% hydrolyzed was supplied by Sigma Aldrich with a molecular weight between 13000 and 23000 and a density of 1.269 g/cm^3. Gd_2O_3:Eu^{3+}, GDO, nanoparticles were obtained from Nanograde and the fluorescence molecules, 2,5 diphenyloxazol (PPO) and (1,4-bis (2-(5-phenioxazolil))-benzol (POPOP) were obtained from Sigma-Aldrich. Ultra-pure water with 18.2 M < SUP > O < /SUP > cm resistivity at 25 °C was obtained from a Millipore Milli-Q system. The commercial scintillator ink EJ296, which was used for benchmarking the performance of the scintillator developed in this work, was supplied by Eljen Technology. All chemicals were used as provided by the suppliers.

2.2. Preparation of the scintillator inks

The scintillator inks were prepared by solvent casting with nanoparticle content of 0, 0.75, and 1,5 wt%. First, the desired amount of GDO and fluorescence molecules, PPO at concentration of 1 wt% and POPOP at concentration of 0.01 wt%, were dispersed in ultra-pure water (18.2 M < SUP > O < /SUP > cm resistivity at 25 °C obtained from a Millipore Milli-Q system) in an ultrasound bath (ATU, Model ATM40-3LCD) for 4 h in order to properly disperse all the fillers. After the dispersion of the nanoparticles, PVA was added and the solution in different polymer/solvent ratios (Table 1) was magnetically stirred and heated at 90 °C, until complete dissolution of the polymer, as reported in [31].

2.3. Preparation of the scintillator films

Scintillator films were prepared both by spray printing and by doctor-blade coating. The PVA films were printed on a PET substrate, in order to obtain flexible scintillators, and dried at 25 °C. The nanocomposite doctor-blade-coated films were prepared on a glass substrate with scintillator nanoparticle content between 0.25 and 1.5 wt% and dried at 25 °C until complete solvent evaporation. These nanocomposites films showed an average thickness of ≈30 μm, measured with gauge Fischer DualScope MPOR. Then, the films were removed from the substrate for characterization.

After the evaluation of the functional performance, films with concentrations of scintillator nanoparticles of 0.75 and 1.5 wt% and produced by spray printing technique were determined to produce the highest visible light output. The nomenclature adopted in the manuscript is as follows: PVA/0.75S-FL means a PVA composite with 0.75 wt % of scintillator fillers and with incorporated fluorescent (FL) molecules.

Table 1
Scintillator inks prepared by varying Gd_2O_3:Eu^{3+} filler content and polymer/solvent relative content.

Ink	GDO content (wt.%)	PVA: water ratio
SC003	0	1:6
SC004	1.5	1:6
SC005	0.75	1:5
SC006	0.75	1:6
SC007	0.75	1:7
SC008	0.75	1:8

2.4. Scintillator films and ink characterization

The morphology of the PVA scintillator films was analyzed by scanning electron microscopy (SEM) (FEI Quanta 650 FEG microscope) with an accelerating voltage of 5 kV. The energy dispersive X-ray (EDX) spectra were measured by an INCA 350 spectrometer (Oxford Instruments) with a primary beam voltage of 20 kV. The rheological behavior of the inks was characterized at 25 °C using a stress controlled rotational rheometer MCR-300 (Anton Paar, Austria) equipped with Couette geometry. After loading the inks into the rheometer, steady shear rates were ramped from 2000 s^{-1} down to 1 s^{-1} within 15 min. This test was immediately followed by another ramp with steady shear rates from 1 s^{-1} up to 2000 s^{-1} also within 15 min. The viscosity data obtained from the two ramps overlapped, indicating that flow curves were obtained under steady state conditions and that the polymer solutions showed no thixotropy.

The optical transmittance of the samples was evaluated by Ultraviolet–Visible spectroscopy (UV-VIS) from 200 to 800 nm with 1 nm steps in a UV-2501PC UV-VIS spectrometer.

For the functional performance of the films, X-ray radiation was projected into the composites and the conversion into visible light was measured. The X-ray radiation was produced using a Bruker D8 Discover diffractometer, using Cu Kα incident radiation, powered with a voltage of 40 kV and a current ranging from 0 to 40 mA (output power ranging from 0 to 1600 W). The efficiency of this conversion was evaluated with a custom-built system that allows quantification of the emitted visible wavelength radiation [31]. Briefly, a light sensor acts as a light-to-frequency converter combining a silicon photodiode and a current-to-frequency converter on a single monolithic CMOS integrated circuit (IC). The sensor response is then read by a Micro Controller Unit (MCU) that saves the data in memory during the irradiation process, and wirelessly transmits them to a remote platform when the process is finished. All measurements were performed in normal atmosphere and at room temperature without encapsulation of the sensors.

3. Results and discussion

3.1. Characterization of the PVA scintillator composites

The morphology of the PVA composite films prepared by doctor-blade technique was studied to test if the addition of the scintillator nanoparticles and fluorescence molecules influences the typical microstructure of PVA as well as to verify if the fillers were well dispersed. Fig. 1 shows SEM images of the pristine PVA sample together with the PVA/0.75S-FL sample, the appearance of which is representative of the other composite samples.

Fig. 1 shows a smooth surface for the pristine PVA films (Fig. 1a) and for the composite (Fig. 1b). Good filler dispersion is observed for the nanocomposite and just a few Gd nanoparticle aggregates are observed at the surface and in the cross-section micrographs (white circles in the inset of Fig. 1d). The EDX measurement revealed the bulk composition of 56 wt% of carbon (C), 43 wt% of oxygen (O) and 0.8 wt% of gadolinium (Gd) for the PVA/0.75S-FL (Fig. 1e). C and most of the O are ascribed to PVA and Gd to the GDO nanoparticles. The amount of Gd estimated by EDX (0.8 wt%) is in good agreement with the amount of Gd_2O_3:Eu^{3+} nanoparticles added to the nanocomposite (0.75 wt%), taking into account that the Gd dominates the content of the nanoparticles by weight. Conversely, Eu doped into GDO nanoparticles at 3 wt% Eu^{3+} was not detected by EDX. EDX mapping revealed a uniform

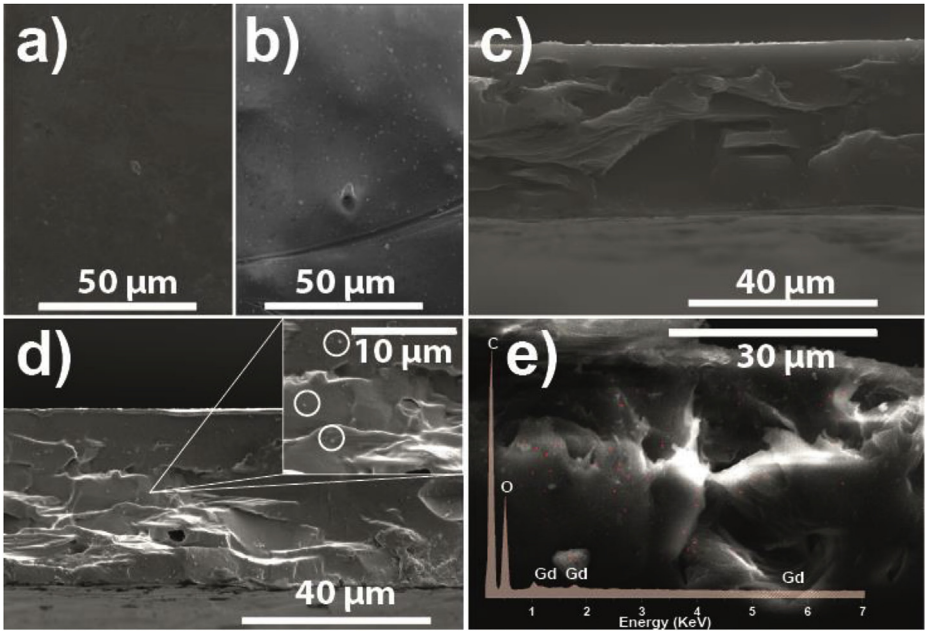

Fig. 1. Surface (a and b) and cross-section (c and d) SEM images of the PVA and PVA/0.75S-FL films, respectively. SEM-EDX mapping and spectrum of the PVA/0.75S-FL film (e).

distribution of the GDO nanoparticles (red dots in Fig. 1e) across the nanocomposite film.

The optical transmittance (Fig. 2a) of the scintillator composites was measured as a function of wavelength and filler content (0, 0.25, 0.5, 0.75 and 1.5 wt%). As expected, the transmittance decreases with increasing filler content in the polymer matrix, while a relatively flat transmittance in the visible range is consistent with the uniform dispersion of the fillers observed by SEM. The inset of Fig. 2a shows the optical transmittance as a function of GDO filler content, at a wavelength of 611 nm, which is the emission peak of the scintillator nanoparticles. For this specific wavelength, the optical transmittance decreases with increasing scintillator filler content from ~90% for the pure polymer down to ~40% for the sample with 1.5 wt% filler content.

The scintillator process taking part in polymer based composites has been presented in [33]. In short: the scintillator process occurs due to the interaction of the X-ray radiation with the scintillator material, which generates a free electron and a deep hole pair excited to the ionization band. Several relaxation processes follow, leading to a large number of relaxed electron-hole pairs which are transferred to lower energy states, accompanied by the corresponding emission of light (Scheme 1). Then, the electrons migrate to the activator excited state and the holes in the valence band migrate to the activator ground state [33]. The transitions of holes and electrons leads to the production of a scintillation photon. The fluorescence molecules (FL) and re-emitted at higher wavelength in the visible wavelength range [34]. Note that large contents of scintillator nanoparticles and fluorescence molecules in the composite lead to higher visible light dispersion and lower scintillator composite performance [27]: increasing filler content leads to increased composite density and higher number of scintillating nanoparticles, leading to an enhancement of X-ray absorption and conversion. On the other hand, it also leads to a decrease in the optical transparency of the polymer-based scintillator composite, due to greater dispersion of light (Scheme 1).

Fig. 2b shows the variation of the efficiency of the X-ray radiation conversion into visible light (visible radiation intensity, termed V.R.I.) as a function of X-ray intensity obtained for the PVA composites prepared with different nanoparticle filler contents by doctor-blade coating. The intensity of the converted visible radiation increases with increasing X-ray output power and small amounts of scintillator GDO nanoparticles, as reported in [31]. The increase of the X-ray power increases the interaction volume, and hence the number of photons produced [9]. The V.R.I. increases with increasing filler content up to 0.75 wt%, presumably because at higher concentrations the increased

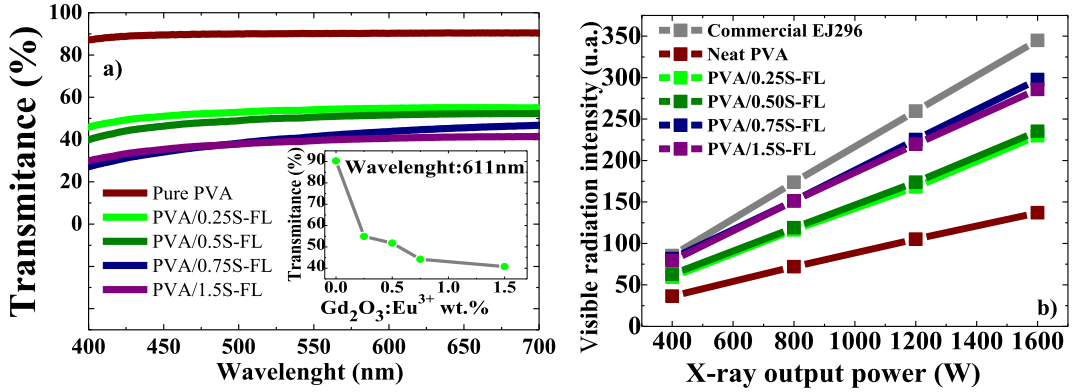

Fig. 2. a) Optical transmitance of the PVA composites as a function of wavelenght and $Gd_2O_3:Eu^{3+}$ content (inset: optical transmittance as a function of $Gd_2O_3:Eu^{3+}$ filler content, at a wavelenght of 611 nm) b) Intensity of the converted visible radiation of the composites as a function of X-ray output power.

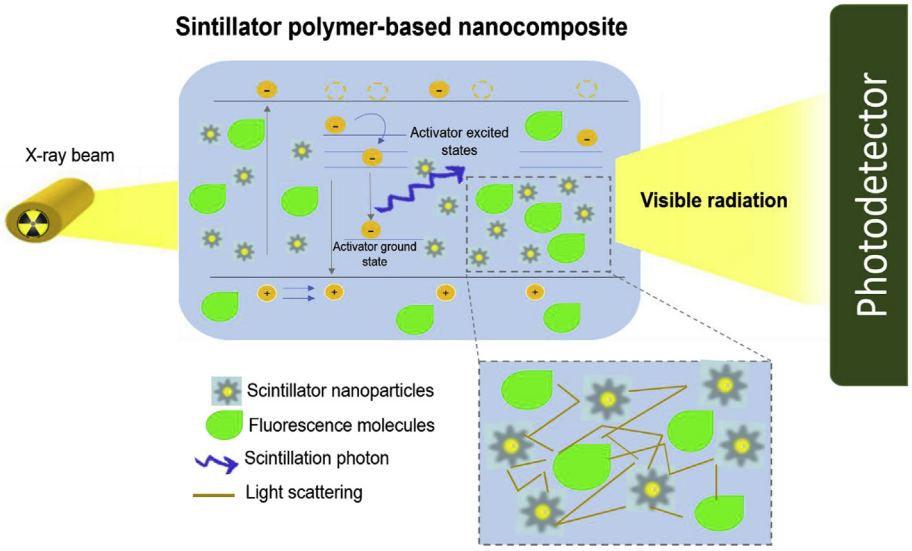

Scheme 1. Schematic representation of the scintillation process induced by X-ray radiation.

conversion of X-ray radiation into visible light is counteracted by the decreasing transmittance in the visible wavelength range [32].

Fig. 2b also shows a commercial scintillator ink, EJ296, for comparison: the PVA nanocomposite scintillator with 0.75 wt% filler content exhibits a response lower only by 14% at the highest X-ray power tested, which would not significantly influence device performance in most applications. As noted above, composites with 0.75 and 1.5 wt% GDO content exhibit similar scintillator performance, accordingly, inks were prepared from these formulations to evaluate their rheology for printing processes.

3.2. Ink characterization

For application and upscaling production of inks, the rheological behavior of the solution is critical because it affects how the ink is transferred to the substrate to form a homogeneous film. The viscosity is affected by various parameters such as temperature, molecular weight of the polymer, solvent, concentration and additives [34]. Thus, viscosity is often used as a quality control parameter of the fluids.

To optimize ink development, the rheological behavior of the suspensions was evaluated. The shear viscosity of PVA suspensions does not exhibit any shear rate dependence (Fig. 3a), indicating classical Newtonian behavior [35]. In fact, the data suggest that this PVA solution is in the dilute regime, because the zero shear viscosity exhibits a linear increase with the PVA volume fraction [36]. The error bars of the extracted zero shear viscosities displayed in the inset of Fig. 3a are large and show that variations in the viscosity of the suspensions are at the limit of torque sensitivity of the rheometer (Couette geometry).

However, a trend for decreasing zero shear viscosity η_o with increasing particle volume fraction is observed. This trend is at odds with the Einstein behavior expected for diluted suspensions of non-interacting hard spheres in a Newtonian solvent with viscosity η_o. Indeed the Einstein relation is represented by equation (1) [37].

$$\eta_0 = \eta_S(1 + 2.5\phi) \quad (1)$$

where ϕ is the volume fraction of spherical particles.

Flocculation between particles could lead to a mismatch between the data and the expected functional dependence, but cannot explain a suspension viscosity smaller than the viscosity of the suspending medium. Indeed, flocculation of silica nanoparticles suspended in PVA suspensions has been recently associated with an increase in η_0, as large particle aggregates are formed through the H-bonding of PVA to the nanoparticles, promoting particle bridging [38]. Thus, to explain the non-Einstein behavior, other types of particle-particle and PVA-particle interactions have to be considered. Indeed, PVA is not fully hydrolyzed (98% of OH groups as reported by the PVA supplier). Accordingly, PVA chains and particles could form complexes: electrostatic repulsion between the few ester groups of the polymer chain is modulated by the

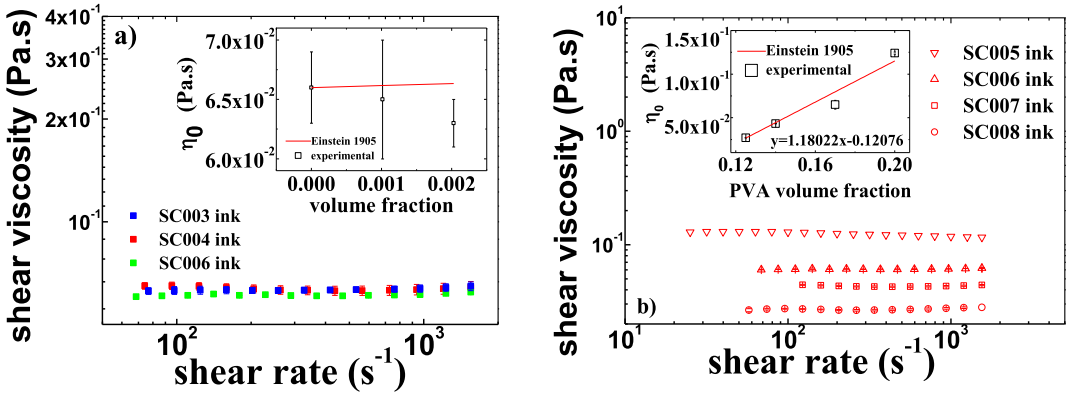

Fig. 3. a) Shear rate dependence of suspensions of Gd2O3:Eu3 + nanoparticles in PVA solution in water. Inset: zero shear viscosity of suspensions as a function of the particle volume fraction. The red line represents the Einstein equation for dilute suspensions of hard spheres; b) Shear rate dependence of 0.75 wt% nanoparticle suspensions in PVA solutions with different PVA concentrations. Inset: zero shear viscosity of suspensions as a function of the PVA concentration. (For interpretation of the references to colour in this figure legend, the reader is referred to the Web version of this article.)

presence of cations available in the solvent. The addition of particles could thus bring a polyelectrolyte effect: the dissociation of protons from the nanoparticles would cause a change in the overall conformation of PVA chain from extended to more coil-like, and result in a decrease in the viscosity of the PVA solution [39].

Adding less PVA in suspensions with a constant volume fraction of particles results in a simple dilution effect of the suspending fluid. This is illustrated in Fig. 3b, where the flow curves of suspensions with different PVA concentrations are reported. All flow curves show Newtonian behavior, indicative of dilute systems. Indeed, the zero-shear viscosity of the suspensions increases linearly with the concentration in PVA, which suggests that no interactions between PVA chains occur, as expected for the dilute regime of a polyelectrolyte solution [38].

Coming back to the non-Einstein behavior suggested by the data reported in Fig. 3a, we note that the adsorption of PVA chains on the surface of particles will effectively reduce the volume fraction of free PVA chains in the suspending medium. As suspensions are diluted and PVA concentration in the solvent remains in the dilute regime, the addition of particles will simply lead to a loss of drag forces between PVA chains and the solvent, thereby reducing the shear viscosity of the suspensions. Rheological data show that all tested formulations exhibit viscosities suitable for doctor-blade application, which is a versatile technique, tolerant of a wide range of viscosities [35]. As far as spraying is concerned, viscosity levels reported in Fig. 3 are within the range of reported values for successful spraying. The rheology of spraying process, however, is far from fully understood. Spraying involves shear rates far above those tested in Fig. 3 and contributions from surface tension, gravity and extensional viscosity. Furthermore, because of the huge shear rates occurring during spraying, issues such as inertial and jetting instabilities cannot be ignored (and cannot be assessed with the rotational rheometer employed in the present study). As a proof-of-concept, a prototype scintillator film was produced by spray printing.

3.3. Deposition of printed scintillator films by spray printing technique

The ink selected for producing the printed active scintillator layer was the SC005 (viscosity of about 0.1 Pa s). The active layer with an average thickness of ≈30 μm was deposited on a PET substrate by spray-printing (Fig. 4a). The adhesion of printed films to substrate was tested to successfully resist removal by the standard tape test, and showed good adhesion between the sprayed films and the PET substrate. The spray-printed film exhibits the same functional performance in the conversion of the X-ray radiation into visible light as the composites obtained by doctor-blade coating. The V.R.I. follows the same trends (results not shown) as the results presented in Fig. 2b.

To evaluate the performance as a scintillator, the film was printed on a photodetector matrix and selectively illuminated by focusing the incident X-ray beam on different photodetectors. An electronic system with RF communication was used to measure all the photodetectors simultaneously, effectively producing a radiation detector with a large area and evaluating the potential of the scintillator film for imaging applications. Fig. 4a shows the schematic representation of the photodetector matrix connected to the RF system [31].

Fig. 4b shows the variation of the visible radiation intensity (V.R.I.) as a function X-ray output power in different photodetectors of the matrix. The V.R.I. shows an increase with increasing X-ray power, analogous to the samples prepared by doctor-blade coating (Fig. 2b). Notably, the printed devices exhibit constant and linear behavior, independently of the selectively illuminated photodetector, indicating good reproducibility of the printing process and uniform dispersion of the fillers. Further, as the scintillator properties depend on the nanoparticles and the fluorescence molecules, and PVA does not suffer degradation on X-ray radiation or at common room temperature conditions, the device shows good stability over time.

Thus, it is demonstrated that an environmentally-friendly scintillator ink based on PVA allows the developed spray printable scintillator composites to be applied for the fabrication of indirect X-ray detectors.

4. Conclusions

A water-based scintillator ink was developed and optimized. The ink formulations include ultrapure water as a solvent and PVA as a binder. The test films were produced by doctor-blade coating and by spray-printing. The printed films were used for the optimization of the

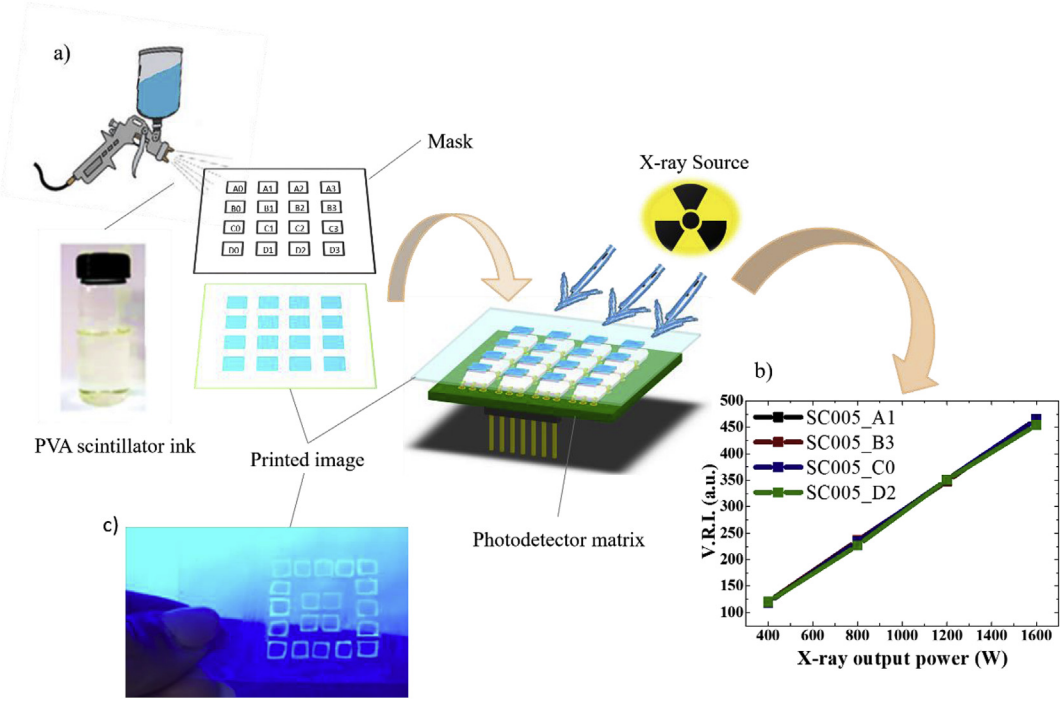

Fig. 4. a) Schematic representation of the construction of the prototype of the spray-printed scintillator film; b) variation of the visible radiation intensity (V.R.I.) as a function X-ray output power in different photodetectors of the matrix, c) Visualization of images printed with water-based scintillator ink.

scintillator filler concentration and showed a homogeneous distribution of scintillator nanoparticles. The rheological characterization of the inks suggests that they behave as Newtonian fluids in the dilute regime. The optimized ink with 0.75 wt% content of scintillator nanoparticles was printed on top of a photodetector matrix as a prototype device, which confirmed a reproducible and linear conversion of the X-ray radiation into visible light by the spray-printed nanocomposite films. This successful prototype device indicates that the ink developed in this work is suitable for the preparation of spray-printed indirect X-ray detectors by a green-solvent approach.

Acknowledgment

The authors thank FEDER funds through the COMPETE 2020 Programme and National Funds through FCT - Portuguese Foundation for Science and Technology under Strategic Funding UID/FIS/04650/2013 and projects PTDC/EEI-SII/5582/2014 and PTDC/CTM-ENE/5387/2014. J.O., P.M.M and V. C. thank the FCT for the SFRH/BD/98219/2013, SFRH/BD/98616/2013 and SFRH/BPD/97739/2013 grants, respectively. The authors acknowledge funding by the Spanish Ministry of Economy and Competitiveness (MINECO) through the project MAT2016-76039-C4-3-R. Financial support from the Basque Government Industry Department under the ELKARTEK program is also acknowledged.

References

[1] S. Lee, J.H. Kim, M. Wajahat, H. Jeong, W.S. Chang, S.H. Cho, J.T. Kim, S.K. Seol, Three-dimensional printing of silver microarchitectures using Newtonian nanoparticle inks, ACS Appl. Mater. Interfaces 9 (2017) 18918–18924.
[2] A. Wisitsoraat, J.P. Mensing, C. Karuwan, C. Sriprachuabwong, K. Jaruwongrungsee, D. Phokharatkul, T.M. Daniels, C. Liewhiran, A. Tuantranont, Printed organo-functionalized graphene for biosensing applications, Biosens. Bioelectron. 87 (2017) 7–17.
[3] C. Tematio, M. Bassas-Galia, N. Fosso, V. Gaillard, M. Mathieu, M. Zinn, E. Staderini, S. Schintke, Design and characterization of conductive biopolymer nanocomposite electrodes for medical applications, Mater. Sci. Forum (2017) 1921–1926.
[4] D.S. Levi, N. Kusnezov, G.P. Carman, Smart materials applications for pediatric cardiovascular devices, Pediatr. Res. 63 (2008) 552–558.
[5] M. Nikl, Scintillation detectors for x-rays, Meas. Sci. Technol. 17 (2006) R37–R54.
[6] A. Quaranta, S.M. Carturan, T. Marchi, V.L. Kravchuk, F. Gramegna, G. Maggioni, M. Degerlier, Optical and scintillation properties of polydimethyl-diphenylsiloxane based organic scintillators, IEEE Trans. Nucl. Sci. 57 (2010) 891–900.
[7] V.N. Bliznyuk, A.F. Seliman, A.A. Ishchenko, N.A. Derevyanko, T.A. Devol, New efficient organic scintillators derived from pyrazoline, ACS Appl. Mater. Interfaces 8 (2016) 12843–12851.
[8] M.C. Righetti, A. Boggioni, M. Laus, D. Antonioli, K. Sparnacci, L. Boarino, Thermal and mechanical properties of PES/PTFE composites and nanocomposites, J. Appl. Polym. Sci. 130 (2013) 3624–3633.
[9] P.M. Martins, P. Martins, V. Correia, J.G. Rocha, S. Lanceros-Mendez, Gd2O3:Eu nanoparticle-based poly(vinylidene fluoride) composites for indirect x-ray detection, J. Electron. Mater. 44 (2014) 129–135.
[10] L. Basiricò, A. Ciavatti, T. Cramer, P. Cosseddu, A. Bonfiglio, B. Fraboni, Direct X-ray photoconversion in flexible organic thin film devices operated below 1 v, Nat. Commun. 7 (2016).
[11] W. Cai, Q. Chen, N. Cherepy, A. Dooraghi, D. Kishpaugh, A. Chatziioannou, S. Payne, W. Xiang, Q. Pei, Synthesis of bulk-size transparent gadolinium oxide-polymer nanocomposites for gamma ray spectroscopy, J. Mater. Chem. C 1 (2013) 1970–1976.
[12] B. Fraboni, A. Ciavatti, L. Basiricò, A. Fraleoni-Morgera, Organic semiconducting single crystals as solid-state sensors for ionizing radiation, Faraday Discuss 174 (2014) 219–234.
[13] Y.S. Zhao, H. Zhong, Q. Pei, Fluorescence resonance energy transfer in conjugated polymer composites for radiation detection, Phys. Chem. Chem. Phys. 10 (2008) 1848–1851.
[14] W.G. Lawrence, S. Thacker, S. Palamakumbura, K.J. Riley, V.V. Nagarkar, Quantum dot-organic polymer composite materials for radiation detection and imaging, IEEE Trans. Nucl. Sci. 59 (2012) 215–221.
[15] P. Martins, Y.V. Kolen'Ko, J. Rivas, S. Lanceros-Mendez, Tailored magnetic and magnetoelectric responses of polymer-based composites, ACS Appl. Mater. Interfaces 7 (2015) 15017–15022.
[16] Y. Wei, S. Chen, F. Li, Y. Lin, Y. Zhang, L. Liu, Highly stable and sensitive paper-based bending sensor using silver nanowires/layered double hydroxides hybrids, ACS Appl. Mater. Interfaces 7 (2015) 14182–14191.
[17] H. Deng, L. Lin, M. Ji, S. Zhang, M. Yang, Q. Fu, Progress on the morphological control of conductive network in conductive polymer composites and the use as electroactive multifunctional materials, Prog. Polym. Sci. 39 (2014) 627–655.
[18] W. Obitayo, T. Liu, A review: carbon nanotube-based piezoresistive strain sensors, Journal of Sensors 2012 (2012).
[19] S. Khan, L. Lorenzelli, R.S. Dahiya, Technologies for printing sensors and electronics over large flexible substrates: a review, IEEE Sensor. J. 15 (2015) 3164–3185.
[20] R.E. Sousa, J. Oliveira, A. Gören, D. Miranda, M.M. Silva, L. Hilliou, C.M. Costa, S. Lanceros-Mendez, High performance screen printable lithium-ion battery cathode ink based on C-LiFePO4, Electrochim. Acta 196 (2016) 92–100.
[21] B.S. Hunter, J.W. Ward, M.M. Payne, J.E. Anthony, O.D. Jurchescu, T.D. Anthopoulos, Low-voltage polymer/small-molecule blend organic thin-film transistors and circuits fabricated via spray deposition, Appl. Phys. Lett. 106 (2015).
[22] D. Khim, K.J. Baeg, B.K. Yu, S.J. Kang, M. Kang, Z. Chen, A. Facchetti, D.Y. Kim, Y.Y. Noh, Spray-printed organic field-effect transistors and complementary inverters, J. Mater. Chem. C 1 (2013) 1500–1506.
[23] A. Mouret, L. Leclercq, A. Mühlbauer, V. Nardello-Rataj, Eco-friendly solvents and amphiphilic catalytic polyoxometalate nanoparticles: a winning combination for olefin epoxidation, Green Chem. 16 (2014) 269–278.
[24] M.I. Baker, S.P. Walsh, Z. Schwartz, B.D. Boyan, A review of polyvinyl alcohol and its uses in cartilage and orthopedic applications, J. Biomed. Mater. Res. B Appl. Biomater. 100 B (2012) 1451–1457.
[25] V.G. Kadajji, G.V. Betageri, Water soluble polymers for pharmaceutical applications, Polymers 3 (2011) 1972–2009.
[26] C. Bao, Y. Guo, L. Song, Y. Hu, Poly(vinyl alcohol) nanocomposites based on graphene and graphite oxide: a comparative investigation of property and mechanism, J. Mater. Chem. 21 (2011) 13942–13950.
[27] O. Kanoun, C. Müller, A. Benchirouf, A. Sanli, T.N. Dinh, A. Al-Hamry, L. Bu, C. Gerlach, A. Bouhamed, Flexible carbon nanotube films for high performance strain sensors, Sensors 14 (2014) 10042–10071.
[28] X. Liu, F. Zhou, M. Gu, S. Huang, B. Liu, C. Ni, Fabrication of highly a-axis-oriented Gd2O3:Eu3+ thick film and its luminescence properties, Opt. Mater. 31 (2008) 126–130.
[29] S.Z. Shmurak, V.V. Kedrov, N.V. Klassen, O.A. Shakhrai, Spectroscopy of composite scintillators, Phys. Solid State 54 (2012) 2266–2276.
[30] R.N. Nurmukhametov, L.V. Volkova, V.G. Klimenko, S.P. Kabanov, R.V. Salov, Fluorescence and absorption of a polystyrene-based scintillator exposed to UV laser radiation, J. Appl. Spectrosc. 74 (2007) 824–830.
[31] J. Oliveira, P.M. Martins, P. Martins, V. Correia, J.G. Rocha, S. Lanceros-Mendez, Gd2O3:Eu3+/PPO/POPOP/PS composites for digital imaging radiation detectors, Appl. Phys. Mater. Sci. Process 121 (2) (1 November 2015) 581–587.
[32] J. Oliveira, P.M. Martins, P. Martins, V. Correia, J.G. Rocha, S. Lanceros-Mendez, Increasing X-ray to visible transduction performance of Gd2O3:Eu3+PVDF composites by PPO/POPOP addition, Compos. B Eng. 91 (2016) 610–614.
[33] S.E. Derenzo, M.J. Weber, E. Bourret-Courchesne, M.K. Klintenberg, The quest for the ideal inorganic scintillator, Nucl. Instrum. Methods Phys. Res. Sect. A Accel. Spectrom. Detect. Assoc. Equip. 505 (2003) 111–117.
[34] M.M. Voigt, R.C.I. Mackenzie, S.P. King, C.P. Yau, P. Atienzar, J. Dane, P.E. Keivanidis, I. Zadrazil, D.D.C. Bradley, J. Nelson, Gravure printing inverted organic solar cells: the influence of ink properties on film quality and device performance, Sol. Energy Mater. Sol. Cell. 105 (2012) 77–85.
[35] H.A. Barnes, J.F. Hutton, K. Walters, An Introduction to Rheology, Elsevier, 1989.
[36] P.G. de Gennes, Scaling Concepts in Polymer Physics, Cornell University Press, 1979.
[37] A. Einstein, Eine neue Bestimmung der Moleküldimensionen, (1905) Buchdruckerei K.J. Wyss.
[38] S. Kim, K. Hyun, B. Struth, K.H. Ahn, C. Clasen, Structural development of nanoparticle dispersion during drying in polymer nanocomposite films, Macromolecules 49 (2016) 9068–9079.
[39] A.V. Dobrynin, R.H. Colby, M. Rubinstein, Scaling theory of polyelectrolyte solutions, Macromolecules 28 (1995) 1859–1871.